METEOROLOGICAL APPLICATIONS
Meteorol. Appl. (2011)
Published online in Wiley Online Library
(wileyonlinelibrary.com) DOI: 10.1002/met.248

RMetS
Royal Meteorological Society

Night time fog detection using MODIS data over Northern India

Sasmita Chaurasia,* V. Sathiyamoorthy, Bipasha Paul Shukla, B. Simon, P. C. Joshi and P. K. Pal

Atmospheric and Oceanic Sciences Group, Space Applications Center, ISRO Ahmedabad-380015, India

ABSTRACT: An algorithm for night time fog detection using satellite data was used to study 2009 and 2010 fog episodes over the North Indian plains. The algorithm employs a bispectral thresholding technique involving brightness temperature difference (BTD) between two spectral channels: 3.9 and 10.75 μm, combining radiative transfer simulations and satellite data. The prolonged fog episode of January 2010 was analysed in detail using this algorithm in conjunction with the meteorological parameters and it was found that upper tropospheric long waves passed over this region during the fog episode. These waves affect the circulation close to the surface and appear to have played an important role in the formation and persistence of fog during 2010. The present thresholding method can be used to monitor night time fog over the Indian subcontinent on an operational basis using the forthcoming geostationary satellite INSAT-3D. Copyright © 2011 Royal Meteorological Society

KEY WORDS fog detection; SBDART; Bi-spectral thresholding

Received 16 May 2010; Revised 14 September 2010; Accepted 17 November 2010

1. Introduction

Fog is one of the meteorological/environmental phenomena which create significant societal and economic problems especially as a major havoc to road and air traffic. Meteorological stations provide information about the fog episodes only on the basis of point observation. Continuous monitoring, as well as a spatially coherent picture of fog distribution, is possible through the use of satellite imagery. In India the entire Indo-Gangetic plains (IG plains) of Northern India is regularly affected by poor visibility in the winter months due to the formation of fog which is brought about by the existence of typical meteorological, environmental and prevailing terrain characteristics of that area (Choudhury *et al*., 2007). On these occasions fog is seen to persist continuously for more than 2 weeks in winter. In the literature, studies of persistent fog episodes on the IG plains are relatively scarce. Some efforts were made earlier to study fog formation on local scales, such as airports in India (Basu, 1952; Natarajan and Banerji, 1959; Mohapatra and Thulsidas, 1998). These suggest that the fog mostly forms in association with 'western disturbances' (eastward moving high and low pressure systems of the upper troposphere) which affect the circulation characteristics close to surface as well. Brij *et al*. (2003) tried to find the reasons behind the occasional persistence of fog condition over the IG plains. They analysed the synoptic conditions during four fog seasons and concluded that fog persists under the synoptic situation that could provide upper air convergence. Fog formation takes place on a synoptic scale. However, its characteristics may change over regional to localized scales depending upon the terrain effects, urban and non-urban regions, availability of water bodies and wet surfaces.

In addition to the large scale circulation, the formation of fog may also be due to a number of other causes. It has been observed that pollution has great influence on the formation of fog in India. The increasing numbers of thermal power plants in the IG plains are contributing towards a higher aerosol concentration, thereby increasing the probability of fog formation (Prasad *et al*., 2006). As aerosols, which act as condensation nuclei, increase in the lower atmosphere, the water vapour present in the atmosphere condenses more effectively due to higher availability of condensation nuclei. Hence, if concentration of aerosols is higher, there will be denser fog and it will last longer.

Even though the hazardous effect of winter fog in the north Indian region is very high it has not been studied extensively. Specifically, its formation, spatial extent and evolution are required to be studied in detail. It is difficult to monitor the spatial and temporal extent of fog over large-scale areas such as the IG plains using a limited conventional and ground based observational network, so satellite based fog monitoring becomes popular due to its enhanced spatial, spectral and temporal resolution and offers new opportunities for real-time fog detection and

* Correspondence to: Sasmita Chaurasia, Atmospheric and Oceanic Sciences Group, Space Applications Center, ISRO, Ahmedabad 380015, India.
E-mail: sasmita@sac.isro.gov.in; sasmita_sac@yahoo.co.in

monitoring using upcoming geostationary satellite such as INSAT-3D. Apart from the use of satellite data (Lee *et al*., 2010) modelling studies can also be carried out for the occurrence of prolonged fog over the Indian region (Choi and Speer, 2006; Shi *et al*., 2010).

In the present study a bi-spectral remote sensing technique for night time fog detection is presented. The study is divided into three parts. The first part deals with the simulation of brightness temperature using two different spectral channels, the 3.9 and 10.75 μm wavelengths analogous to the MODIS (MODerate Resolution Imaging Spectroradiometer) Middle Infrared (MIR) and Thermal Infrared (TIR) channels to find out a threshold for the identification of fog using satellite data. The second part of the study involves the determination of the same threshold from the satellite data and implementation of the threshold for the detection of fog over the IG plains during two fog episodes, (1) around 21 December 2008 to 8 January 2009, and, (2) around 1–25 January 2010. The third part presents the large scale circulations that prevailed during the January 2010 fog episode. This work has been carried out as a baseline study which will be applied for the monitoring/detection of fog from INSAT-3D on an operational basis in the future.

2. Data used

Night time fog detection has been carried out using the MODIS data. The MODIS sensor on board the EOS TERRA and AQUA platforms shows the best spectral resolution from operational Low Earth Observation (LEO) systems with 36 spectral bands from visible to thermal infrared portion of the electromagnetic spectrum (29 spectral bands with 1 km, 5 spectral bands with 500 m and 2 spectral bands with 250 m nadir pixel dimensions (Schueler and Barnes, 1998; Levy *et al*., 2007)).

Daily horizontal winds, temperature and relative humidity data from the NCEP-NCAR reanalysis dataset (Kalnay *et al*., 1996) available at 2.5° latitude × 2.5° longitude resolution are used to study the large scale weather conditions associated with fog episodes. NCEP-NCAR reanalysis outputs are divided into four classes (classes A–D) depending upon the degree to which they are influenced by the model and observation. The zonal and meridional wind components come under class A (strongly influenced by observations) whereas humidity and surface temperature come under class B (both observation and model have strong influence). Class C

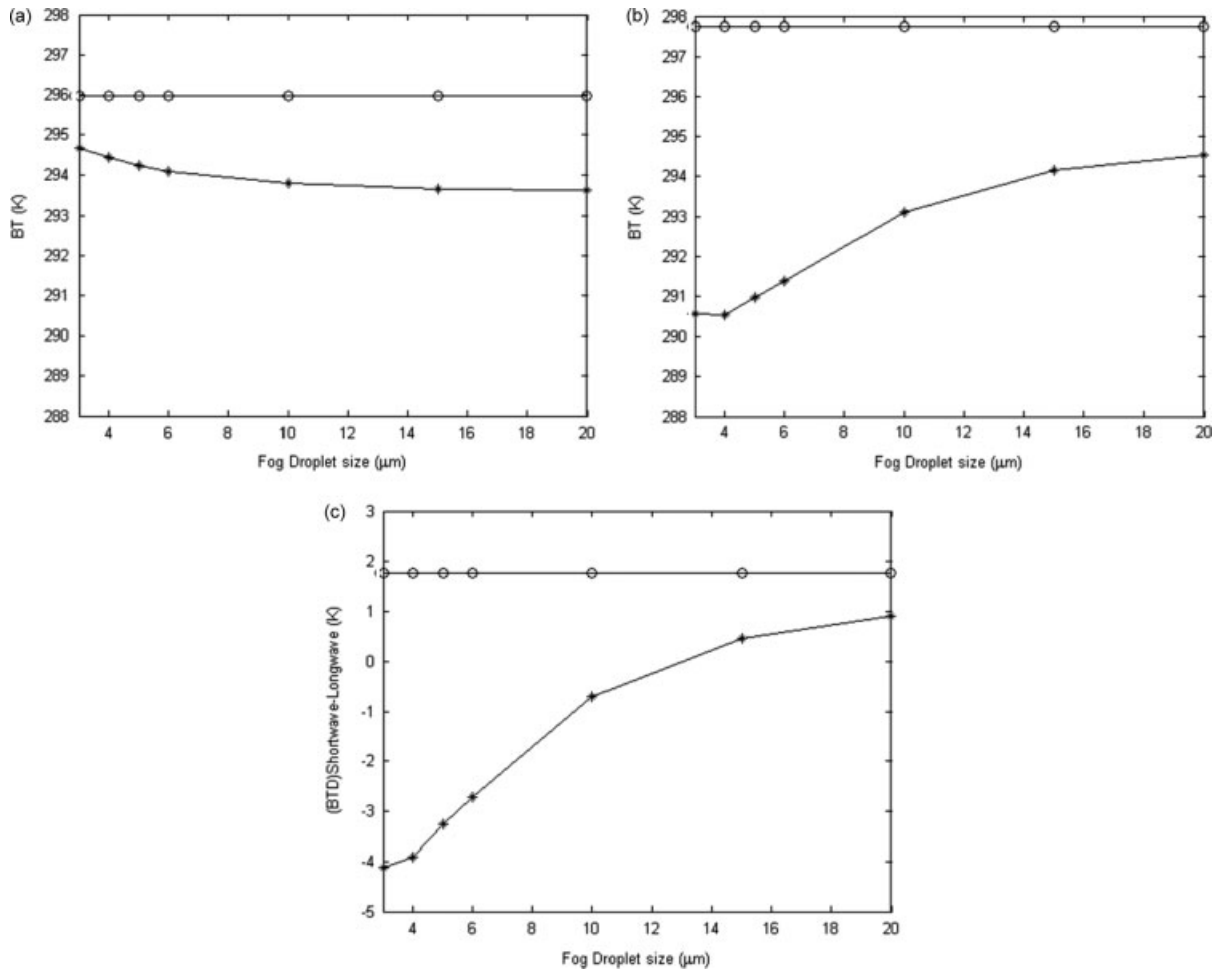

Figure 1. Variation of brightness temperature (K) with fog droplet size (μm) for (a) TIR channel 10.8 μm (b) MIR channel 3.9 μm (c) MIR-TIR channel during night (—✳— fog, —⊖— no fog).

indicates that there are no observations directly affecting the variables, so that it is derived solely from the model. Class D represents a field that is obtained from climatological values.

The Indian Space Research Organisation, (ISRO) maintains a large network of surface meteorological observatories equipped with Automatic Weather Stations (AWSs) over India. They record surface meteorological parameters every hour which are then transmitted to the Meteorological and Oceanographic Data Archival Center (MOSDAC) located at the Space Applications Center, Ahmedabad (www.mosdac.gov.in). The surface observations from the AWS, were used to verify the fog that occurred over IG plains during 2010 fog episode.

3. Methodology

3.1. Radiative transfer simulation for fog detection thresholds

Detection of fog using satellite channels is often carried out using the brightness temperature difference (BTD) image of the 3.9 and the 10.75 μm channels. This technique is especially successful for the night time fog detection when the emissivity of fog is lower compared to all other clouds due to the similarity of 3.9 μm wavelength and mean fog droplet size (Bendix *et al*., 2004).

The first step in fog detection is to determine thresholds for typical fog/low stratus. Although some thresholds are employed for fog detection in different parts of the world (Ellrod, 1995; Lee *et al*., 1997), an attempt has been made to identify a suitable threshold for the IG plains using radiative transfer (RT) calculations for the 3.9 and 10.75 μm channels. The purpose of this is twofold. First, this exercise gives an idea about the sensitivity of the brightness temperature to different fog properties (fog droplet size, optical depth and height). Second, this provides a base for the simulations for daytime fog detection, which is quite challenging owing to the solar contribution in the 3.9 μm wavelength that reduces the BTD between the two channels.

The RT simulations for this study are carried out using the RT code Santa Barbara DISORT Atmospheric Radiative Transfer (SBDART). SBDART is a combination of a sophisticated discrete ordinate radiative transfer module, with a low-resolution atmospheric transmission model,

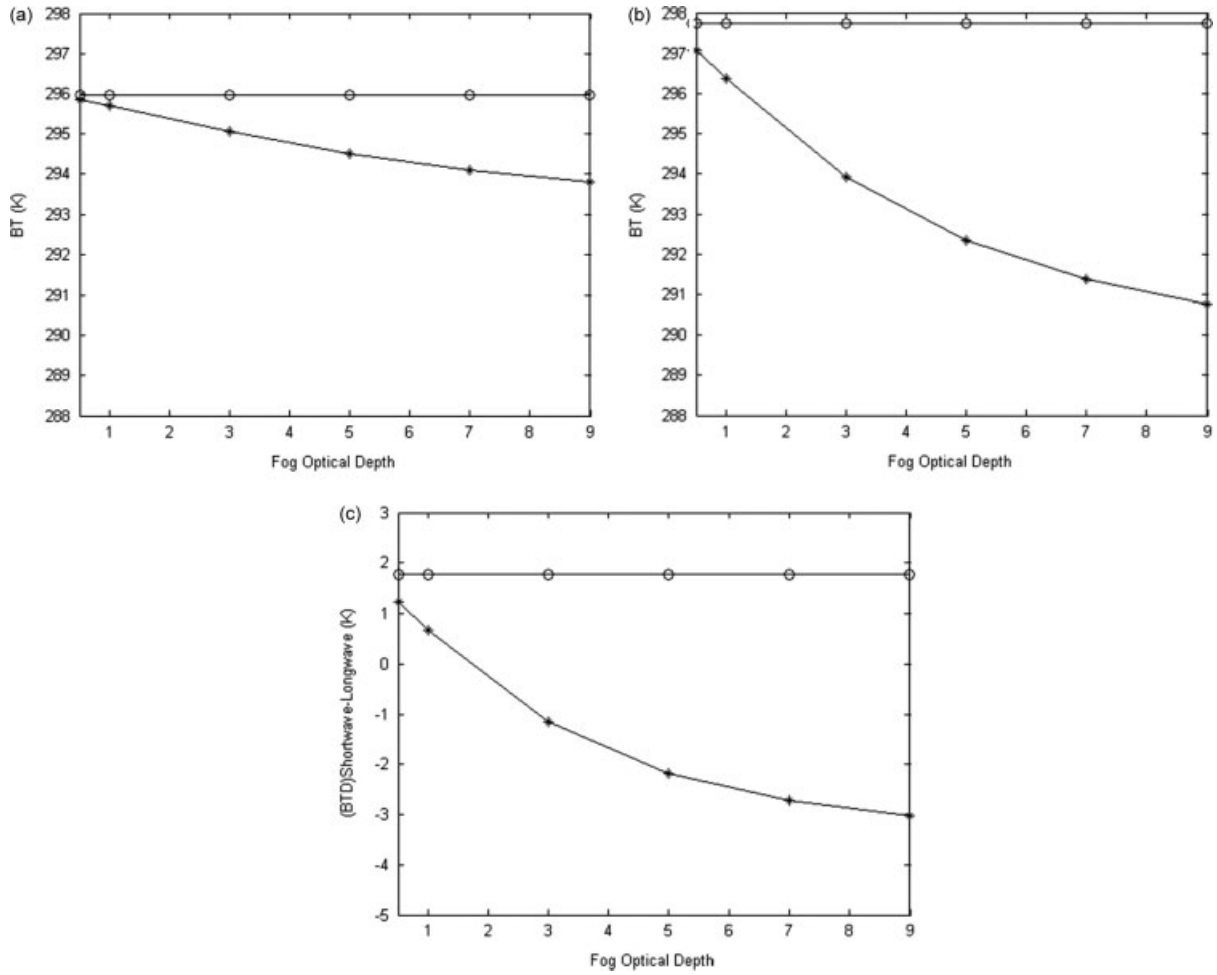

Figure 2. Variation of brightness temperature (K) with fog optical depth for (a) TIR channel 10.8 μm, (b) MIR channel 3.9 μm (c) MIR-TIR channel during night (—✳— fog, —⊖— no fog).

and is designed for analysis of a wide variety of RT problems encountered in satellite remote sensing.

In SBDART, the RT equations are numerically integrated with the Discrete Ordinate Radiative Transfer (DISORT) module (Stamnes *et al.*, 1988). This method uses a numerically stable algorithm to solve the equations of plane-parallel radiative transfer in a vertically inhomogeneous atmosphere (Ricchiazzi *et al.*, 1998). In SBDART, the intensity of scattered and thermally emitted radiation can be computed at different directions and heights. Computations can be performed up to 65 atmospheric layers and 40 radiation streams. The radiative processes included in the model are Rayleigh scattering, gaseous absorptions, cloud and aerosol scattering and absorptions. The computation of radiative transfer in a cloudy atmosphere requires knowledge of different scattering parameters, which are computed in SBDART using a Mie-scattering code for spherical cloud droplets with statistical distribution of drop radius.

3.2. Satellite data pre-processing

The MODIS level 1B data for night time over north India were obtained from http://ladsweb.nascom.nasa.gov for 21 December 2008 to 8 January, 2009 around 2000 UTC and from 30 December 2009 to 28 January 2010 around 1630 UTC within a time range of 1 h, because the formation of fog is initiated in the night. The level 1B emissive channels were geo-registered and the data corresponding to 3.9 μm (Band 22 of MODIS channels) and 10.75 μm (Band 31 of MODIS channels) were extracted. The radiance values of both channels were converted to brightness temperature following Planck's function:

$$BT = \frac{C_1}{\lambda \left\{ \log \left(\left(\frac{C_2 \lambda^{-5}}{I_\lambda} \right) + 1 \right) \right\}} \qquad (1)$$

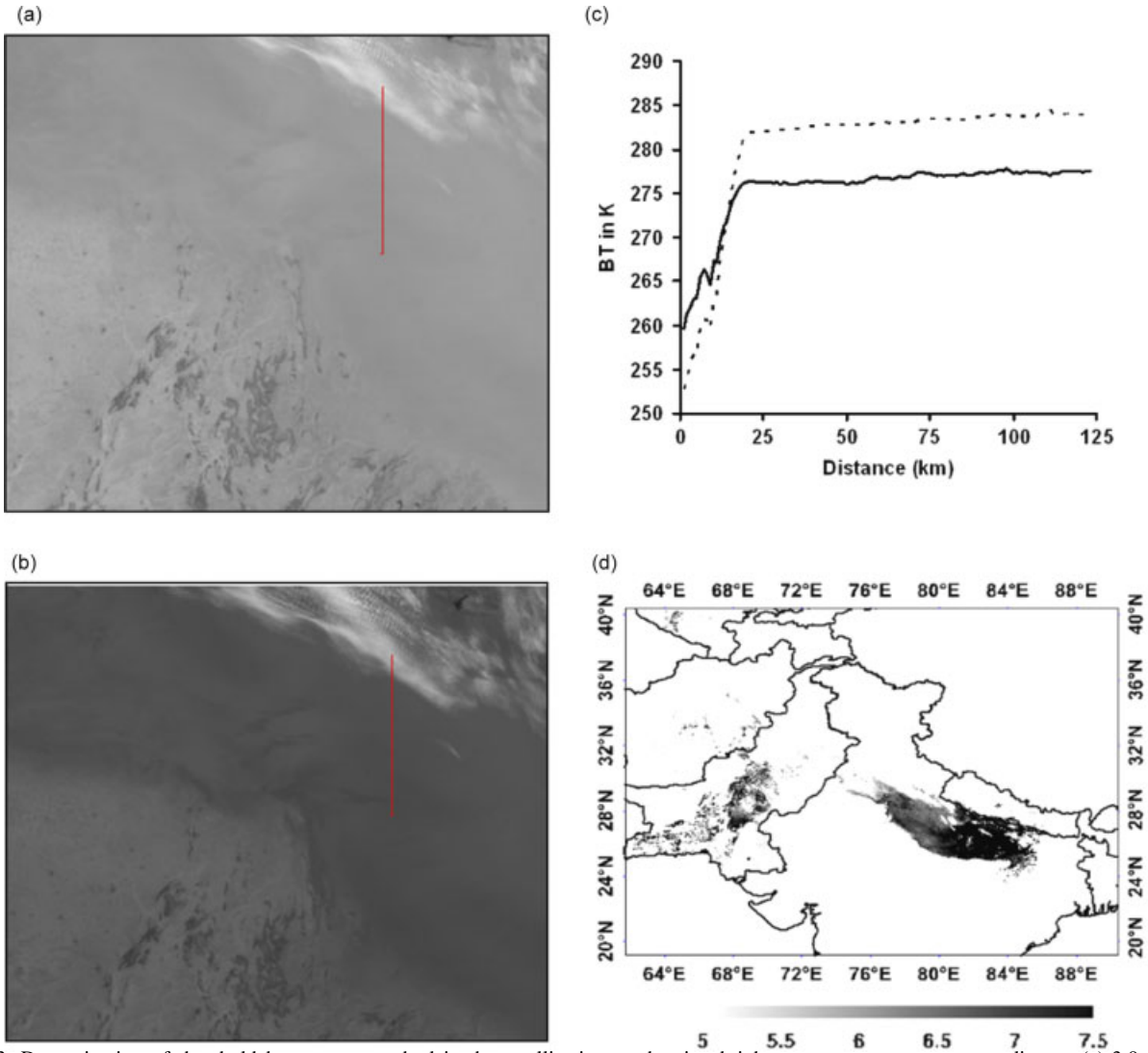

Figure 3. Determination of threshold by transact method in the satellite image showing brightness temperature corresponding to (a) 3.9 μm channel, (b) 10.8 μm channel, (c) variation of brightness temperature corresponding to 3.9 μm channel (solid line) and 10.8 μm channel (dotted line) along a transect (vertical line on the satellite data), (d) detection of fog using the threshold. This figure is available in colour online at wileyonlinelibrary.com/journal/met

where, $C_1 = 14\,387.7$ μmK, $C_2 = 1.19104 \times 10^8$ Wμm^4 m^{-2}sr^{-1}, and I_λ is the radiance.

3.3. Detection of fog using satellite data

The difference of brightness temperature corresponding to the two channels is analysed as an indication for the presence of fog. The theoretical basis for the detection using the 3.9 μm channel and the 10.75 μm channel rely on the particular emissive properties of the two channels for fog droplets (Bendix and Bachmann, 1991). The small droplets found in fog are less emissive at 3.9 μm than at 10.75 μm, whereas both emissivities are roughly the same for larger droplets (Hunt, 1973). The difference between brightness temperatures measured at both wavelengths is tested against a threshold value and attributed to the categories of low stratus/clear/other cloud. The method has been successfully implemented on the Geostationary Operational Environmental Satellite which provides the required spectral bands (Ellrod, 1995; Wetzel *et al*., 1996; Lee *et al*., 1997; Greenwarld and Christopher, 2000; Underwood *et al*., 2004). Recently, Cermak and Bendix (2007) have applied the same algorithm to data of the Spinning Enhanced Visible and Infrared Imager (SEVIRI) on board the Meteosat Second Generation (MSG).

4. Results and discussion

4.1. SBDART Simulations for night time fog

For radiative transfer of fog, the parameters which are considered are the height of fog layer, its optical thickness and droplet size. In SBDART, the height of cloud layers (km) may be specified as separate cloud layers or as range of height, which will be filled by cloud. In the present study, since it was observed from the literature that standard fog height ranges from ground to approximately

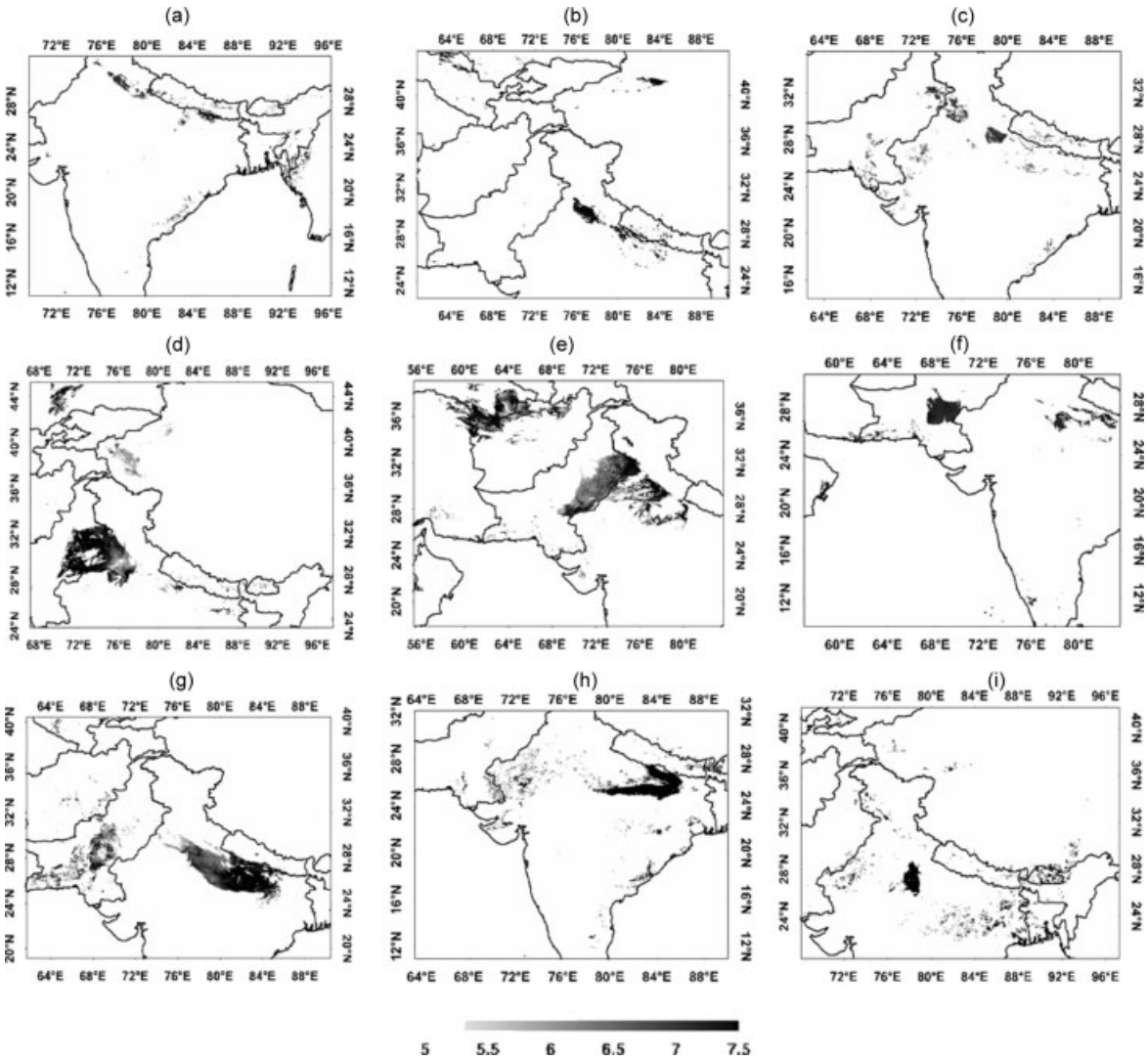

Figure 4. Evolution of night time fog over IG plains from 23 December 2008 to 06 January 2009 monitored using present threshold method (a) 23 December 2008 2020 UTC, (b) 24 December 2008 2100 UTC, (c) 26 December 2008 2050 UTC, (d) 28 December 2008 2035 UTC, (e) 29 December 2008 2120 UTC, (f) 31 December 2008 2110 UTC, (g) 2 January 2009 2055 UTC, (h) 4 January 2009 2045 UTC, (i) 6 January 2009 2030 UTC.

50 m, a single layer at surface level is simulated. The optical depths are available from different experimental observations (Bendix, 2002; Lu and Niu, 2008). It is found that fog optical depth ranges up to 30, with a modal count of $\tau = 8$.

Effective radius, which is defined as the ratio of second and third moments of radius distribution, is a measure of fog droplet size. Field measurements show that a narrow droplet distribution with small radii is associated with radiation fog while a broader, sometimes double-peak, spectrum is typical for advection fog (Pinnick *et al*., 1979). In general, the frequency distribution of effective radius is slightly asymmetric with modal count of $r_e = 6$ μm. The other major parameters, which are modified for SBDART simulation, include atmospheric profiles, surface albedo and solar zenith angle.

For the present study, atmospheric profiles given by the SBDART tropical model atmosphere have been used, which provide pressure, temperature, humidity and ozone density at different atmospheric layers for typical tropical climatic conditions. Secondly, for specifying surface albedo features, the Hapke Analytic Bidirectional Reflection Distribution Function (BRDF) model for vegetation has been employed, which uses a non-Lambertian surface reflectance. Thirdly, since night time fog is being simulated, solar input is turned off by setting solar zenith angle $>90^{\circ}$. Details of the SBDART simulation configuration modified for the current study are provided in Table I.

The results of the simulation study are presented in Figures 1 and 2. In Figure 1(a–c), change of brightness temperature (BT) with fog droplet size (effective radius) is illustrated for TIR, MIR and their difference respectively. A reference level of BT for non-foggy clear conditions is also plotted. Here the optical depth is assumed to be seven as obtained from experimental observations. It can be seen that with increase in fog droplet size there is a slight decrease in BT for TIR

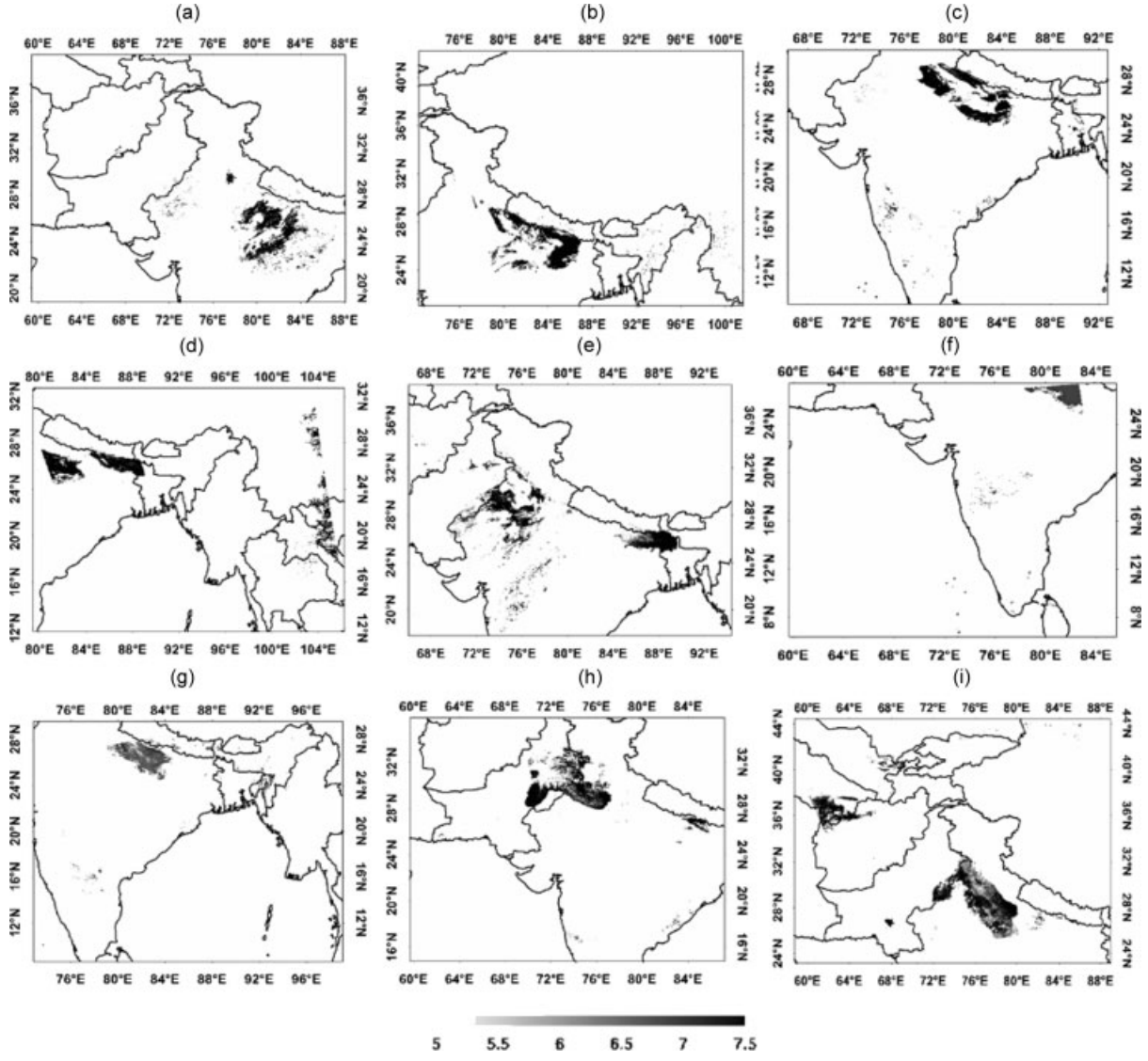

Figure 5. Night time fog as detected by bi-spectral method using MODIS data from 30 December 2009 to 8 January 2010 (a) 30 December 2009 1710 UTC, (b) 31 December 2009 1615 UTC, (c) 1 January 2010 1655 UTC, (d) 2 January 2010 1600 UTC, (e) 3 January 2010 1645 UTC, (f) 4 January 2010 1725 UTC, (g) 5 January 2010 1630 UTC, (h) 6 January 2010 1715 UTC, (i) 8 January 2010 1705 UTC.

channel while for MIR channel BT increases rapidly, whereas no change is seen when there is no fog. Thus, the BTD of these two channels is higher (∼4 K) for small droplet size and decreases rapidly as drop size increases.

Similarly, variation of BT with fog optical depth is illustrated in Figure 2, for a fog effective radius of 6 μm. As expected it can be seen that for optically dense fog the BTD between the two channels is higher. Hence it can be concluded that optically thin fog or fogs with greater effective radius such as maritime fog do pose a difficulty in detection. Since at present the concern is mainly with radiation fog, which is associated with droplet size distribution peaking near small radii, simulation shows feasibility of fog detection using threshold methods.

4.2. Threshold for night time fog detection using satellite data over IG plains

The threshold for night time fog detection for a particular episode under study has been found out by studying the variation of brightness temperature in both 3.9 and 10.75 μm bands for different features of the image

Table I. Details of SBDART configuration.

S. no	Parameter	Description
1	Central wavelength	10.75 (TIR), 3.9 (MIR)
2	Atmospheric parameters	Tropical model atmosphere including vertical profiles of pressure and temperature having constant water vapour density of 2.9 g cm^{-2}
3	Surface albedo feature	Specified by Hapke analytic BRDF model with the parameters 1. Single scattering albedo = 0.101 2. Asymmetry factor of scattering = 0.263 3. Magnitude of hot spot = 0.589 4. Width of hot spot = 0.046 corresponding to generic vegetation
4	Fog base	0 m
5	Optical depth (range)	0–9
6	Droplet size (range)	2–20 μm
7	Output specification	Radiance at nadir at 100 km

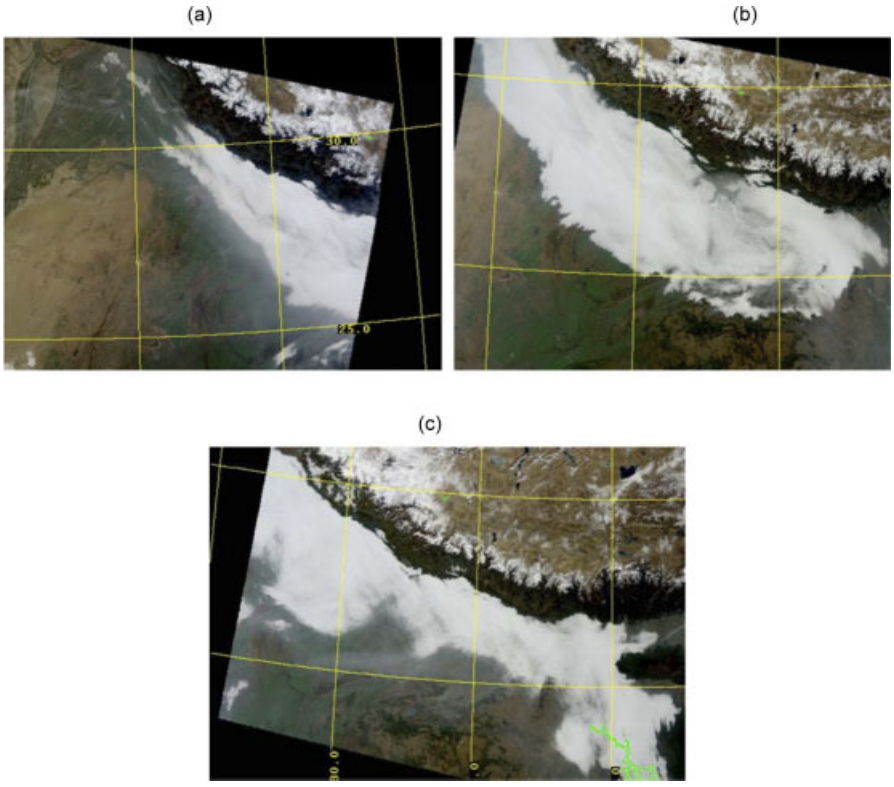

Figure 6. Fog episode of 2010 as seen in the day time visible images of MODIS (a) 1 January 2010 0600 UTC, (b) 2 January 2010 0505 UTC, (c) 4 January 2010 0450 UTC. This figure is available in colour online at wileyonlinelibrary.com/journal/met

i.e. dense fog, cirrus cloud and cloud free regions over the IG plains. Figure 3 shows the variation of brightness temperature in both the channels along a transect (vertical line AB) drawn from the cirrus cloud to the dense fog. A large difference between the brightness temperatures signifies the presence of fog or low to middle level clouds. From the figure it is clearly seen that a brightness temperature difference threshold of 5–7.5 K can detect fog with reasonable accuracy over the IG plains. Using the same threshold, the night time fog over IG plains has been detected and shown in Figures 4 and 5.

The threshold of 4 K, as obtained from the simulation study and discussed in the earlier sections is less than the threshold which has been observed using the satellite data. This may be due to the fact that in the IG plain the fog may be denser implying a larger optical depth and small droplet size.

4.3. Identification of fog in satellite images

Using a constant BTD threshold of 5–7.5 K between the 3.9 μm and 10.75 μm channels, the evolution of the fog episode from 21 December 2008 to 8 January 2009 and around 1 January to 25 January 2010 has been studied. The evolution of fog for the two episodes are shown in Figures 4 and 5 respectively.

From Figure 4 it is seen that on 23 December 2008 there were small patches of fog over northern India which gradually intensified and covered the entire IG plains on 2 January 2009. After 2 January 2009 it started dissipating.

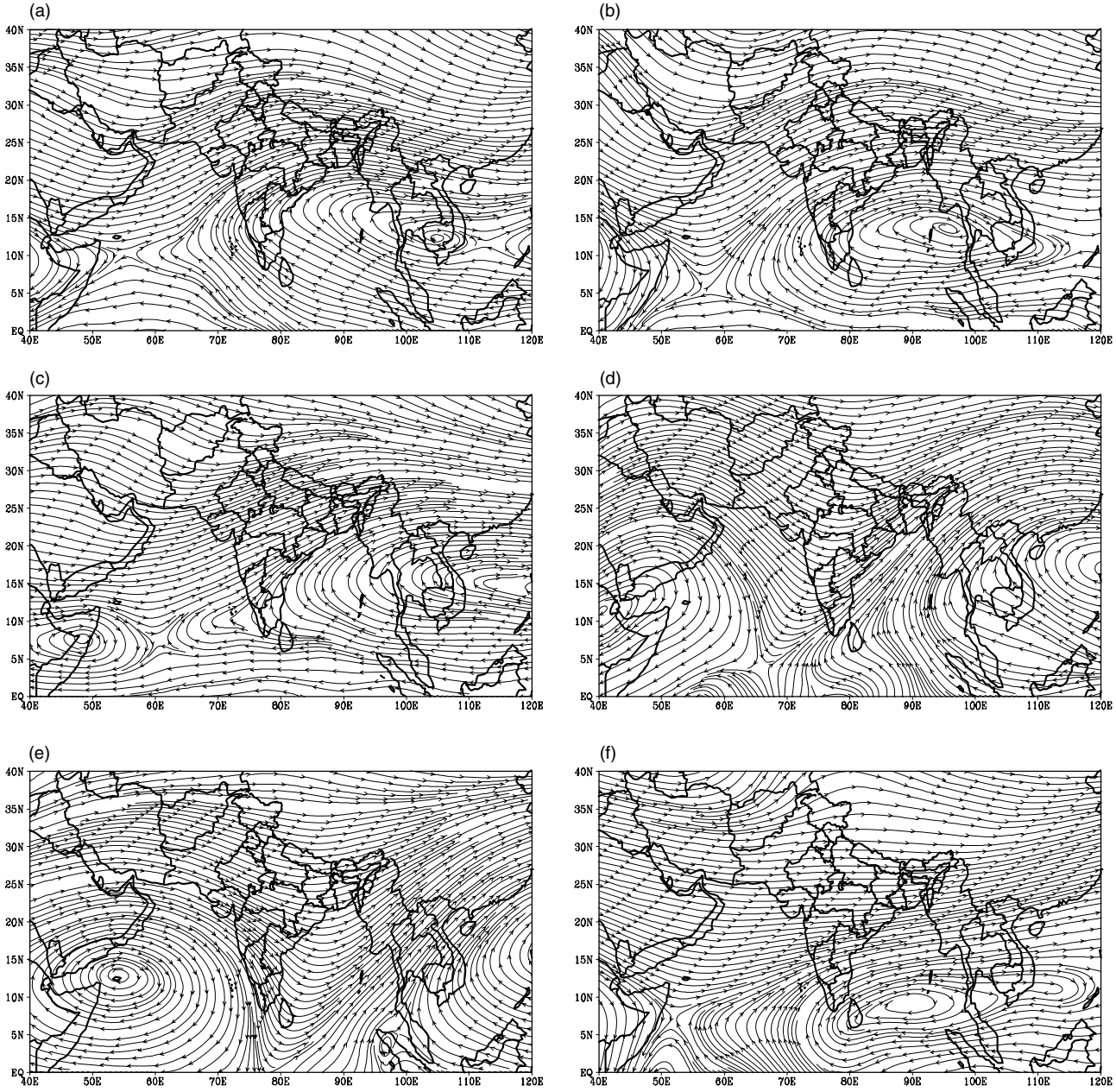

Figure 7. Five-day average stream lines at 300 hPa during 1–30 January 2010.

The second case presents a prolonged fog episode of IG plain that stretched over a period of nearly 1 month. It started around 30 December 2009 and severely reduced the visibility in this region causing several train accidents. It also caused delay in the train and air schedules and hampered normal living conditions. The day to day evolution of fog for the first half of the fog episode is shown in Figure 5. It is observed from the figure that on 30 December, 2009 fog is detected over the northern region, gradually it covered the entire IG plains and persisted until 25 January 2010. This can also be confirmed from the day time visible images of MODIS (Figure 6).

4.4. Synoptic condition associated with the prolonged fog episode of 2010

4.4.1. Large scale circulation during 1–30 January 2010

The 5 day average streamlines at 300 hPa from 1 to 30 January 2010 are shown in Figure 7. A trough over Saudi Arabia in the first week of January slowly moved eastward until 25 January and dissipated later on. It can be seen from the figure that the trough has deepened between 16 and 25 January, stretched meridionally between the equator and the IG plain. The southerly winds in the eastern parts of the trough line transport

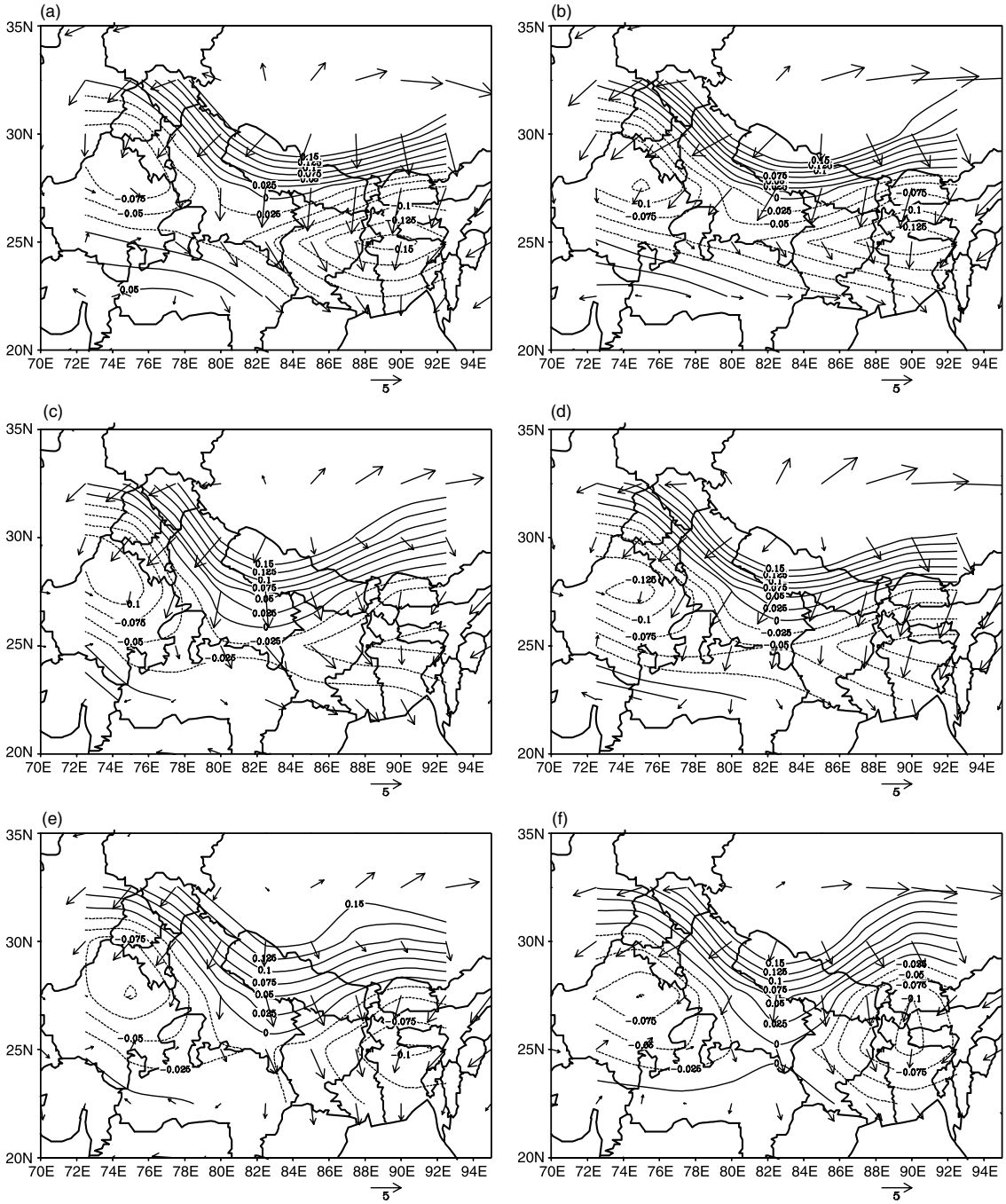

Figure 8. Five-day average horizontal divergence ($\times 10^4$) s^{-1} and wind (m s^{-1}) at 925 hPa during 1–30 January 2010.

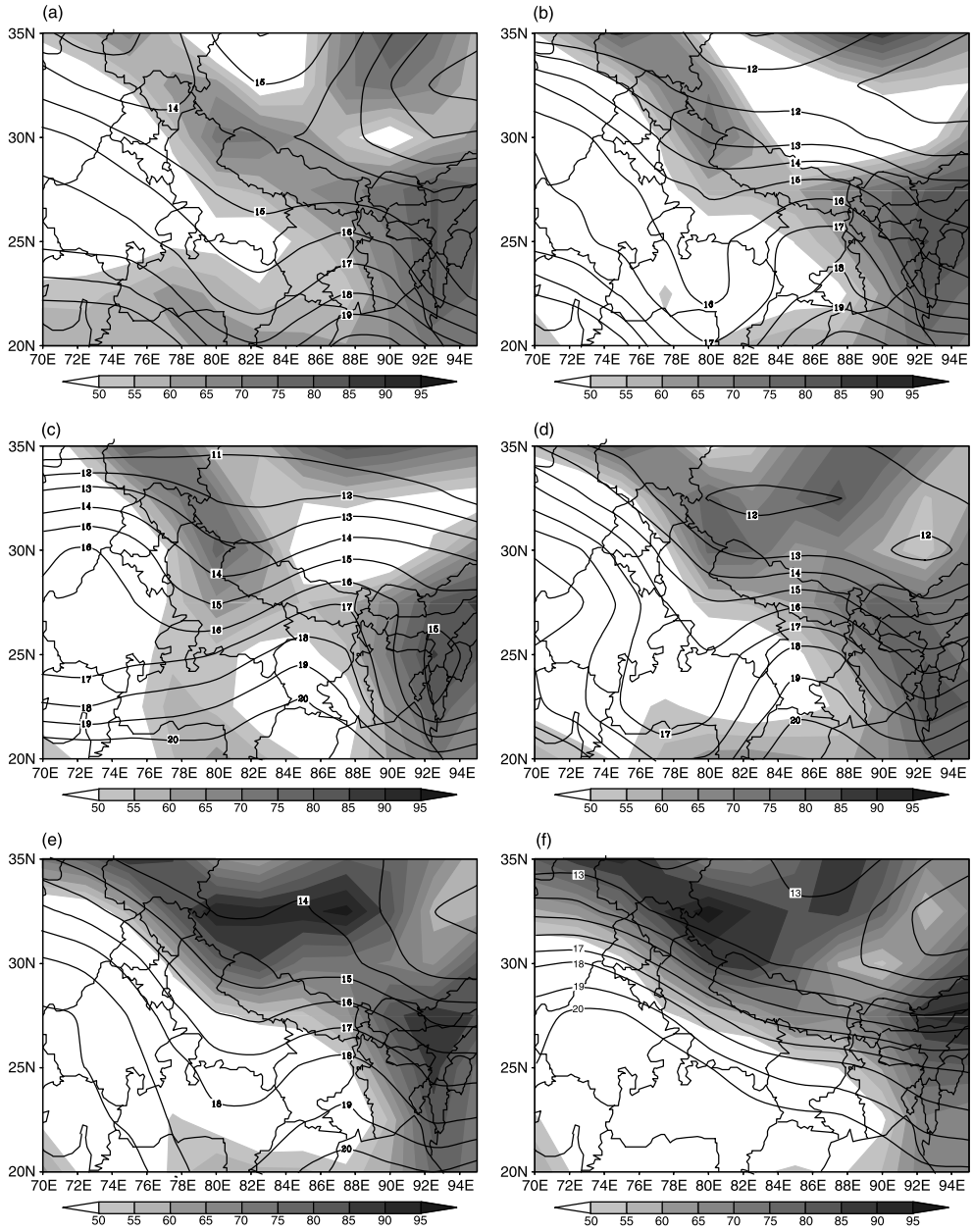

Figure 9. Five-day average temperature (°C) and relative humidity (%) at 1000 hPa during 1–30 January 2010.

warm and moist air from the equatorial latitudes to IG plains, while the northwesterly winds in the western parts of the trough bring colder air from the middle latitudes to India. The upper level cyclonic circulation associated with the trough is expected to generate upper level convergence and lower level divergence. In Figure 8, the 5 day average divergence and horizontal winds near to surface (925 hPa) are shown for 1–30 January 2010. Over the IG plains, mild to strong divergence is seen during the initial 25 days. The surface winds appear to be relatively weaker during this period. In Figure 9, relative humidity and temperature contours averaged at 5 day intervals during 1–30 January 2010 are shown. The increased relative humidity and lower temperatures at the lower levels suggests that the moist air from the south and cold air from the north in the upper/middle troposphere are brought to the lower levels by the upper level convergence-lower level divergence pattern (Figure 8). The close matching of the divergence contours and relative humidity contours also confirms this transport. The already moist-cold lower levels of the IG plains (by local evaporation and evapotranspiration due to extensive cropping practices) become more moist and cold by this downward transport. The lower level divergence and associated stable atmospheric conditions inhibit the convective activity. The moist, calm, cold and clear sky conditions in the IG plains favoured the fog formation in January 2010. The quasi-permanent nature of this trough helped the fog to persist for about 1 month over IG plains. The Himalayas traps the moist and cold air and helps the fog formation. Once the trough dissipated around 26–30 January 2010 the fog also disappeared due to the arrival

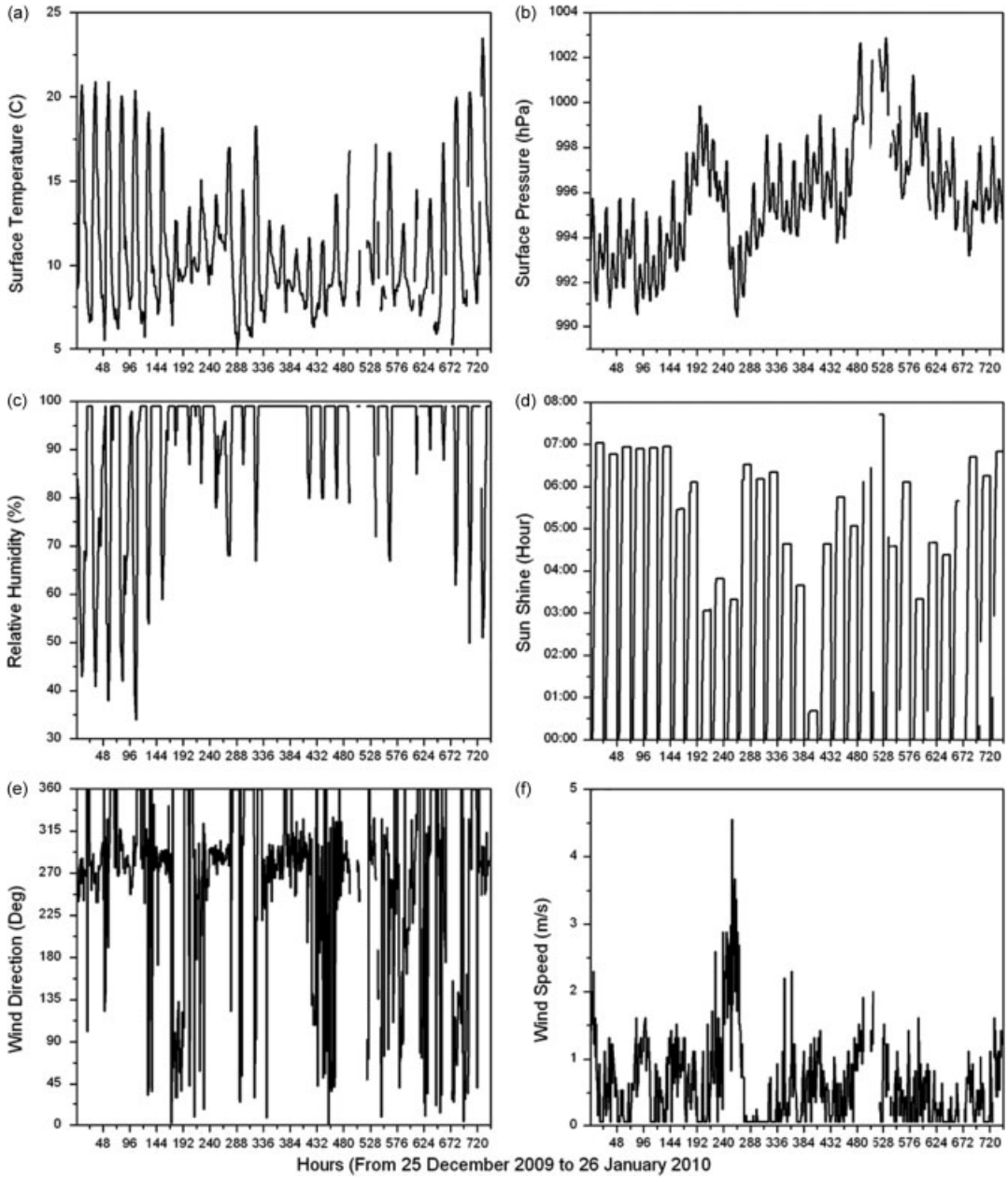

Figure 10. Surface meteorological parameters over Narora, UP (India) from 25 December 2009 to 26 January 2010.

of lower level cyclonic circulation and associated unstable atmospheric conditions.

4.4.2. Observation of fog episode with AWS observations

An example of AWS observations made by an AWS located at the centre of the IG plains, Narora (lat 28°9′N, lon 78°24′E) is shown in Figure 10. Daily evolution of the six surface meteorological parameters: surface temperature, surface pressure, relative humidity, sunshine hour, wind direction and wind speed over the location, are shown in the figure. A striking feature is that a sudden change is observed in these parameters during and after the fog episode. The surface temperature has decreased and relative humidity has increased, showing the persistence of fog between 1 January 2010 and 25 January 2010. The surface pressure showed the arrival of a high pressure system followed by low pressure indicating the passage of western disturbance during the fog episode. The sunshine hours also decreased considerably during the fog episode. The winds are relatively calm and are frequently from the west during the intense fog episode. All these variations in surface parameters from the AWSs confirm the fog persistence for a long period and the association between western disturbance and fog formation.

5. Conclusions

Night time fog detection using a bi-spectral, thresholding technique involving the brightness temperature difference between two spectral channels (3.9 and 10.75 μm) was

studied using radiative transfer simulation as well as satellite data. The night time fog detection using the two MODIS channels centred around 3.9 and 10.75 μm were encouraging. It successfully detected the night time fog for the 2009 and 2010 winter seasons over the IG plains. The prolonged fog episode of 2010, which disrupted rail, road and air traffic in the IG plains, was found to be closely associated with the passage of upper tropospheric waves called western disturbances over the IG plains during this period.

The present thresholding method can be successfully used to monitor fog in real time by using data from the forthcoming geostationary satellite INSAT-3D. However, in future, the threshold value of observed brightness temperature difference between cloud and cloud-free areas will be determined dynamically. During daytime, however, the situation is entirely different due to similar spectral behaviour of snow, fog and other water clouds in the visible bands and the contamination of the 3.9 μm band by solar radiation (Bendix and Bachmann, 1991). The solar signal that mixes into 3.9 μm radiation renders the method useless after sunrise, as the small fog droplets reflect at this wavelength. Therefore, an altogether different approach is needed for day time fog detection.

References

Basu SC. 1952. Fog forecasting over Calcutta and neighborhood. *Indian Journal of Meteorology and Geophysics* **3**(4): 281–289.

Bendix J. 2002. A satellite-based climatology of fog and low-level stratus in Germany and adjacent areas. *Atmospheric Research* **64**: 3–18.

Bendix J, Bachmann M. 1991. A method for detection of fog using AVHRR-imagery of NOAA satellites suitable for operational purposes. *Meteorologische Rundschau* **43**: 169–178 (in German).

Bendix J, Cermak J, Thies B. 2004. New perspectives in remote sensing of fog and low stratus – TERRA/AQUA-MODIS and MSG. In *Proceedings of the Third International Conference on Fog, Fog Collection and Dew*. University of Pretoria: Cape Town, South Africa; G2.1–G2.4.

Brij B, Trivedi HK, Bhatia RC. 2003. On the persistence of fog over northern parts of India. *Mausam* **54**: 4851–4860.

Cermak J, Bendix J. 2007. Dynamical night time fog/low stratus detection based on Meteosat SEVIRI data – a feasibility study. *Pure and Applied Geophysics* **164**: 1179–1192.

Choi H, Speer MS. 2006. The influence of synoptic-mesoscale winds and sea surface temperature distribution on fog formation near the Korean western peninsula. *Meteorological Applications* **13**: 347–360.

Choudhury S, Rajpala H, Sarafa AK, Panda S. 2007. Mapping and forecasting of North Indian winter fog: an application of spatial technologies. *International Journal of Remote Sensing* **28**: 3649–3663.

Ellrod GP. 1995. Advances in the detection and analysis of fog at night using GOES multi spectral infrared imagery. *Weather Forecasting* **10**: 606–619.

Greenwarld TJ, Christopher SA. 2000. The GOES I-M imagers: new tools for studying microphysical properties of boundary layer stratiform clouds. *Bulletin of American Meteorological Society* **81**: 2607–2619.

Hunt GE. 1973. Radiative properties of terrestrial clouds at visible and infra-red thermal window wavelengths. *Quarterly Journal of Royal Meteorological Society* **99**: 346–369.

Kalnay E, Kanamitsu M, Kistler R, Collins W, Deaven D, Candin L, Iredell M, Saha S, White G, Woollen J, Zhu Y, Chelliah M, Ebisuzaki W, Higgins W, Janowiak J, Ropelewski KC, Mot C, Wang Leetmaa A, Reynolds R, Roy J, Joseph D. 1996. The NCEP/NCAR 40 year reanalysis project. *Bulletin of American Meteorological Society* **77**: 437–471.

Lee J, Park JU, Cho J, Baek J. 2010. A characteristic analysis of fog using GPS-derived integrated water vapour. *Meteorological Applications* **17**(4): 463–473, DOI: 10.1002/met.182.

Lee TF, Turk FJ, Richardson K. 1997. Stratus and fog products using GOES-8-9 3.9 μm data. *Weather Forecasting* **12**: 664–677.

Levy RC, Remer LA, Mattoo S, Vermote E, Kaufman YJ. 2007. Second-generation operational algorithm: retrieval of aerosol properties over land from inversion of moderate resolution imaging specroradiometer spectral reflectance. *Journal of Geophysical Research* **112**: D13211. DOI: 10.1029/2006JD007811.

Lu C, Niu S. 2008. Study on Microphysical characteristics of winter fog in Nanjing Area, China. *Proceedings of the International-Workshop on Geoscience and Remote Sensing*, Shanghai, China, **1**: 273–276.

Mohapatra M, Thulsidas A. 1998. Analysis and forecasting of fog over Bangalore Airport. *Mausam* **49**(1): 135–142.

Natarajan G, Banerji RC. 1959. Fog over Agartala airfield. *Indian Journal of Meteorology and Geophysics* **10**(2): 161–168.

Pinnick RG, Jennings SG, Chy'lek P, Auvermann HJ. 1979. Verification of a linear relation between IR extinction, absorption and liquid water content of fogs. *Journal of Atmospheric Sciences* **36**: 1577–1586.

Prasad AK, Singh RP, Kafatos M. 2006. Influence of coal based thermal power plants on aerosol optical properties in the Indo-Gangetic basin. *Geophysical Research Letters* **33**: L05805.

Ricchiazzi P, Yang S, Gautier C, Sowle D. 1998. SBDART: a research and teaching software tool for plane-parallel radiative transfer in the earth's atmosphere. *Bulletin of the American Meteorological Society* **79**: 2101–2114.

Schueler CF, Barnes WF. 1998. Next generation MODIS for polar operational environmental satellites. *Journal of Atmospheric and Ocean Technology* **15**: 430–439.

Shi C, Yang J, Qiu M, Zhang H, Zhang S, Li Z. 2010. Analysis of an extremely dense regional fog event in Eastern China using a mesoscale model. *Atmospheric Research* **95**: 428–440.

Stamnes K, Tsay S, Wiscombe W, Jayaweera K. 1988. Numerically stable algorithm for discrete-ordinate-method radiative transfer in multiple scattering and emitting layered media. *Applied Optics* **27**: 2502–2509.

Underwood SJ, Ellrod GP, Kuhnert AL. 2004. A multiple-case analysis of nocturnal radiation-fog development off California utilizing GOES night time fog product. *Journal of Applied Meteorology* **43**: 297–311.

Wetzel MA, Borys RD, Xu LE. 1996. Satellite microphysical retrievals for land based fog with validation by ballon profiling. *Journal of Applied Meteorology* **35**: 810–829.

